CORROSION SCIENCE AND TECHNOLOGY, Vol.23, No.6(2024), pp.538~545 pISSN 1598-6462 / eISSN 2288-6524
[Research Paper] DOI: https://doi.org/10.14773/cst.2024.23.6.538

Study on Characteristics and Mechanism of Blackening Behavior Under Anti-Fingerprint Coatings of Al-Zn-Mg Coated Steel Sheet

Yuling Ren[1†], Lin Lu[2], Kai Wang[1], Chuanhua Lin[1], Xinyan Jin[1], and Hongwei Qian[1]

[1]*Baoshan Iron and Steel Co., Ltd., Shanghai, 200941, China*
[2]*University of Science and Technology Beijing, Beijing, 100083, China*
(Received January 25, 2024; Revised April 14, 2024; Accepted April 15, 2024)

Fingerprint resistant sheets with a substrate of 55%Al-Zn-Mg coated steel are prone to blackening under service environment. In this study, the chromatic aberration of each 55%Al-Zn-Mg coated steel sheet sample was characterized with a colorimeter. Corrosion morphologies and chemical compositions of blackening samples were observed with a scanning electron microscope coupled with an energy dispersive spectroscope (SEM-EDS). Corrosion products generated from different alloy phases of the Al-Zn-Mg coating were analyzed by micro-Raman spectroscopy. The black area of the blackened sample formed corrosion products including needle shaped products $Zn_5(OH)_6(CO_3)_2.H_2O$ and spherical corrosion products $Al(OH)_3$. In addition, the blackening mechanism of the Al-Zn-Mg coating was thoroughly discussed based on scanning Kelvin probe force microscopy (SKPFM) results. The $MgZn_2$ phase and the Zn-rich phase in the Al-Zn-Mg coating had lower Volta potentials than the Al-rich phase in neutral electrolytes. This might have preferentially corroded the anode of corrosion micro-cells. The resulting corrosion products underneath the anti-fingerprint coating finally induced the blackening phenomenon.

Keywords: *55%Al-Zn-Mg coated steel, Anti-fingerprint coating, Blackening behavior, Underneath corrosion, Volta potential*

1. Introduction

The chromium free fingerprint resistant aluminum zinc magnesium coated steel plate (AZM), with a plating solution composition of 55% aluminum-41% zinc- 2% Mg, is prone to local black discolorations, as shown in Fig. 1. AZM coating is consist chiefly of rich aluminum phase, rich zinc phase, as well as Mg_2Si and $MgZn_2$ phases, as shown in Fig. 2. The island like $MgZn_2$ phase is embedded in the middle of the rich zinc phase, and the rich zinc phase is divided into two types based on zinc contents. The white phase is named rich zinc phase - H, and the light gray phase is named rich zinc phase - L.

As reported in literature, an improper production process and a moistening of the steel plates during transportation, storage under humid and hot conditions may induce blackening. In this paper, the blackened sample and the normal sample were characterized with a scanning electron microscope coupled with energy dispersive spectroscopy (SEM-EDS), Raman spectroscopy and a scanning Kelvin probe force microscopy (SKPFM), based on which the blackening mechanism of AZM coating was investigated.

1.1 Sample and Testing Method

The blackened sample is shown in Fig. 3, which comes from an application site. During the stacking and storage of fingerprint-resistant steel plates coated with AZM,

Fig. 1. The photo of black discoloration phenomenon on the surface of aluminum zinc magnesium coating

†Corresponding author: Ren_yl@baosteel.com

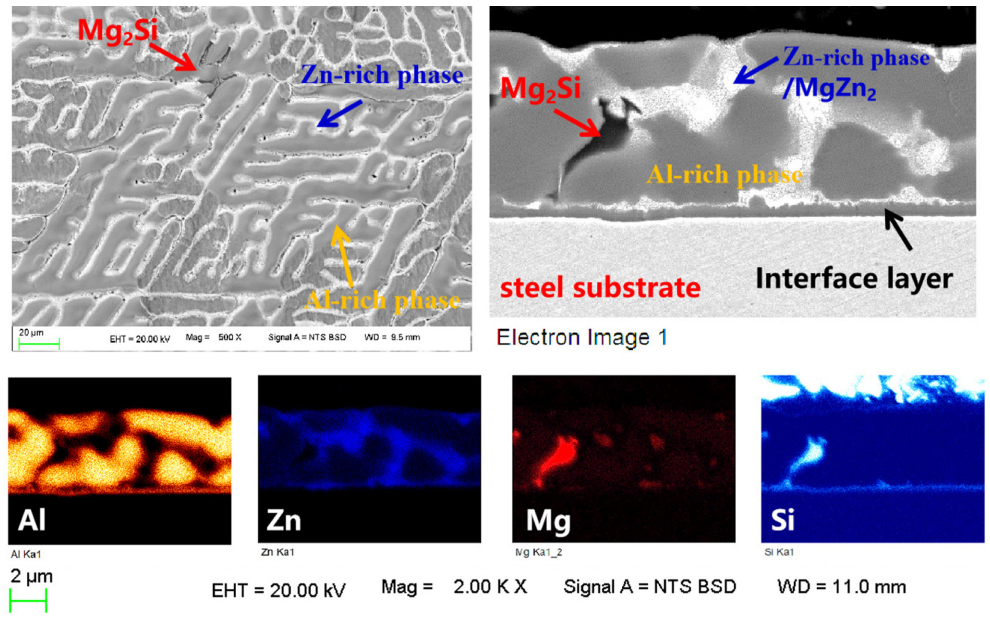

Fig. 2. Phase structure of aluminum zinc magnesium coating

Fig. 3. The photo of the blackening sample plate

localized blackening was observed on the surface of the steel plates under a wetting condition.

Using a colorimeter (Color Eye XTH, USA), the color difference between the blackened sample and the normal sample was measured.

A scanning electron microscopy (GeminiSEM 500, Zeiss, UK) equipped with an energy dispersive X-ray spectroscopy (EDS; Aztec Xmax 50, Oxford, UK) was used to observe the surface and cross-sectional morphology of the sample, as well as the composition.

In situ analysis of corrosion products on the blackened sample was conducted with a micro-Raman spectrometer (HORIBA Jobin Yvon, Japan). And detections of Volta potential for different alloy phases in AZM coating was conducted with a SKPFM (Multimode 8, Bruker Nano Inc., USA).

3. Results and Analysis

3.1 Chromatic aberration resulting from blackening

Using a normal sample as a standard, chromatic aberrations were measured on the white and black areas of the blackened sample respectively, and the results was listed in Table 1. The color difference for the black area of the blackened sample is very high, with an average ΔE* of 13.20, and the color difference for the white area is close to1.24, and thus the visual color difference between the two area is large. Another main difference is ΔL * value, and the black area manifested with negative values, resulting in a black appearance to naked eyes.

Table 1. Color difference of blackened sample

Sample	Zone	ΔL*	Δa*	Δb*	ΔE*	AVE ΔE*
A	white	1.78	-0.33	0.27	1.83	1.24
		-0.30	0.19	0.36	0.51	
		1.28	-0.36	0.41	1.39	
A	black	-13.16	0.35	2.14	13.34	13.20
		-13.59	0.41	2.30	13.79	
		-12.30	0.33	1.94	12.46	

Table 2. Composition of control sample plating

Sample	site	Al (at%)	Zn (at%)	Mg (at%)	O (at%)	Substance
Normal	1	72.7	12.43	0.75	14.12	Al-rich phase
	2	53.58	22.2	3.65	20.57	Zn-rich phase

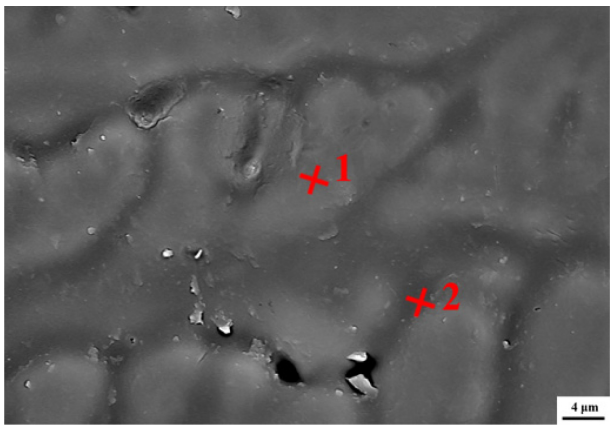

Fig. 4. Control sample surface morphology

3.2 Microscopic morphology and composition of blackened samples

Microscopic surface morphology observation and EDS composition analysis were conducted on the white and black areas of the fingerprint-resistant steel plate, and the normal sample were used as a control. The normal sample coating mainly includes zinc-rich and aluminum-rich phases (Fig. 4, Table 2), and EDS results showed an uniform surface oxygen distribution (Fig. 5).

Correspondingly, the same analysis were conducted on the black and white areas of the blackened sample (Fig. 6, Table 3). It can be seen that the aluminum rich and

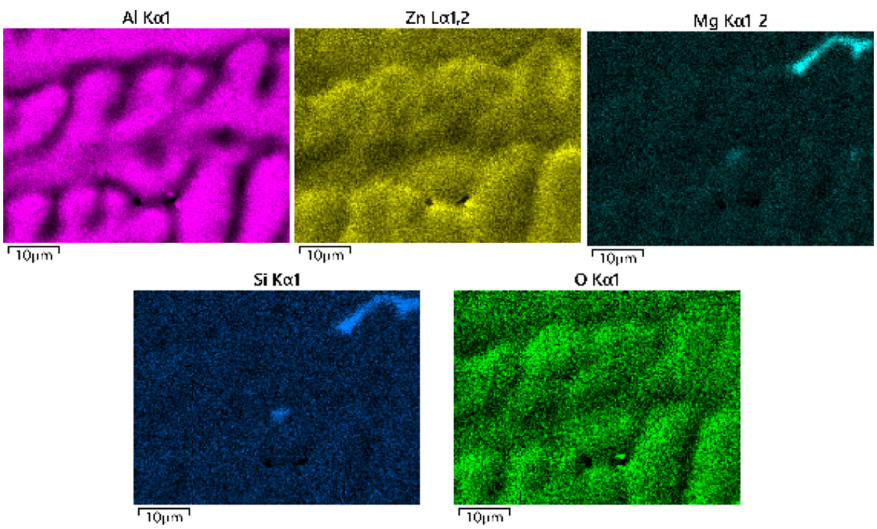

Fig. 5. Distribution of normal sample composition surface

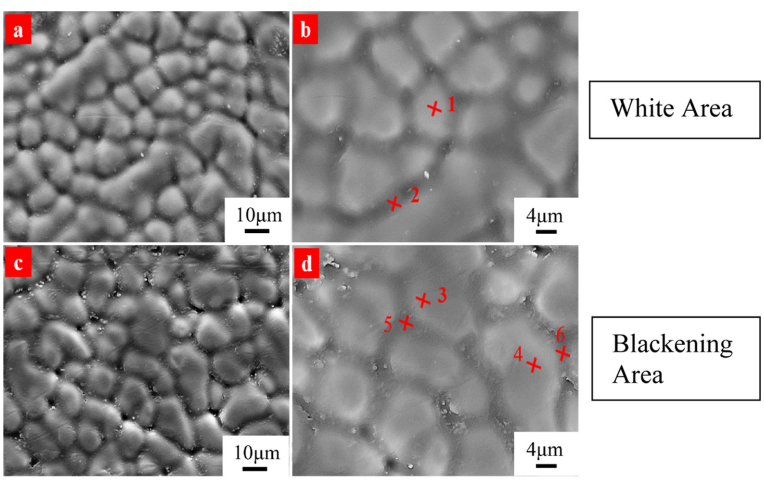

Fig. 6. Surface morphology of the black and white areas of the blackened sample

Table 3. Composition of plating in different areas of blackened sample

Zone	Location	Al (at%)	Zn (at%)	Mg (at%)	O (at%)	substance
White	1	61.99	15.54	0.63	21.84	Al-rich phase
	2	37.99	35.88	1.58	24.55	Zn-rich phase
Black	3	43.68	6.76	0.96	48.6	blackening Al-rich phase
	4	67.16	15.34	0.78	16.72	Al-rich phase
	5	35.61	8.02	1.28	55.09	blackeningZn-rich phase
	6	38.78	35.99	1.42	23.81	Zn-rich phase

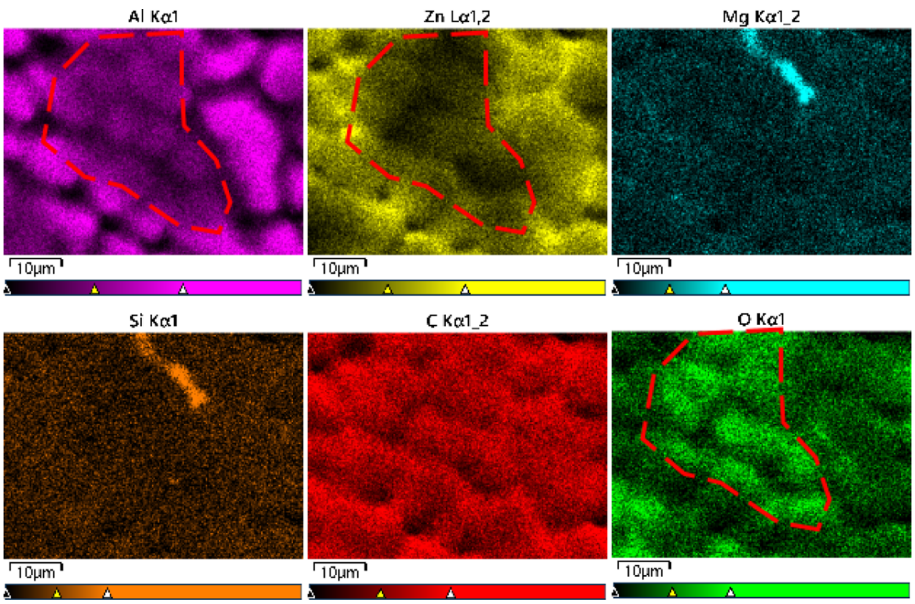

Fig. 7. Composition surface distribution of blackened sample

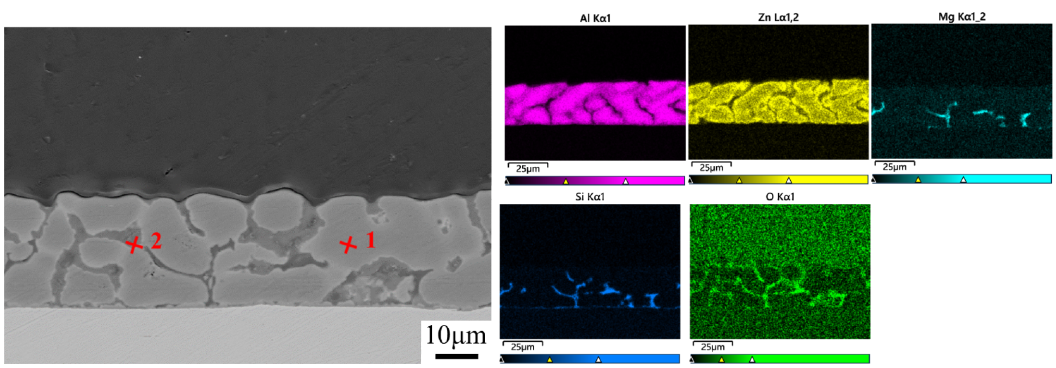

Fig. 8. Cross section morphology and composition distribution of the white area

zinc rich phases in the white area both contain certain amounts of oxygen, which are 21.84% and 24.55%, respectively. The oxygen content is higher than 14.12% and 20.57% of the normal sample. A much higher oxygen content was observed for the alloy phases in the heavily blackened part with the value of 48.6% and 55.09%, respectively, indicating that the surface blackening of AZM coating is attributed to an oxidation of the alloy phase. In the element mapping results (Fig. 7), it is evident that the oxygen enrichment is directly related to the reduction of Al and Zn elements.

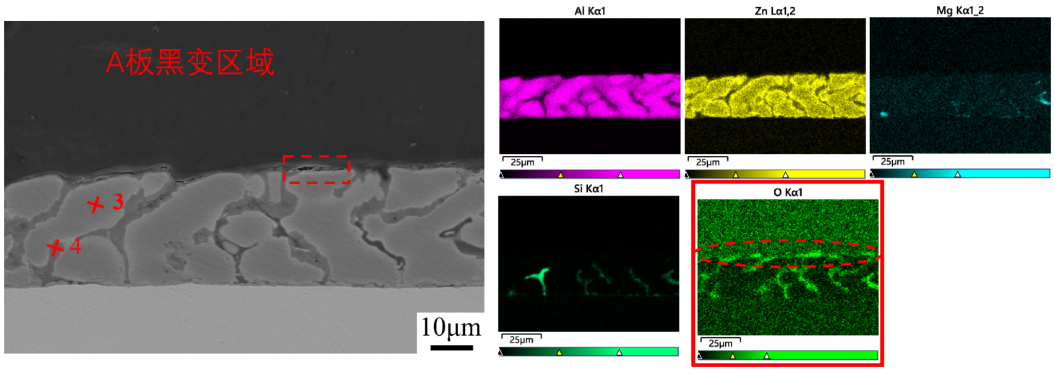

Fig. 9. Cross section morphology and composition distribution of the black area

Table 4. Composition differences between different phases in the white and black areas of the blackened sample

Zone	Location	Al (at%)	Zn (at%)	Mg (at%)	O (at%)	substance
White	1	87.7	9.34	0.69	2.28	Al-rich phase
	2	66.4	12.01	0.92	20.67	Zn-rich phase
Black	3	87.77	9.49	0.63	2.1	Al-rich phase
	4	71.89	10.98	0.27	16.86	Zn-rich phase

3.3 The cross-sectional morphology and composition of the blackened sample

Based on the observation of cross-sectional microstructure and the composition detection of the coating in the black and white areas (Fig. 8, Fig. 9, Table 4), it was found that the magnesium content in the zinc-rich and aluminum-rich phases in the black area was lower than that in the white area. In EDS element mapping results, it was also observed that the magnesium distribution in the black area was lower than that in the white area, indicating that magnesium preferentially dissolved during the blackening process.

In addition, it was observed in Fig. 9 that corrosion products were presented at the interface between the plating layer and the fingerprint resistant film (the area in the red frame), which is right above the aluminum-rich phase. The thickness of the black product layer at this point is about 1 μm. Comparing its morphology and composition with the corrosion product of aluminum (Fig. 10) it can be inferred that the corrosion product is mainly composed of spherical aluminum oxides, indicating that the aluminum rich phase has corroded here and caused the delamination of the fingerprint resistant film from AZM coating.

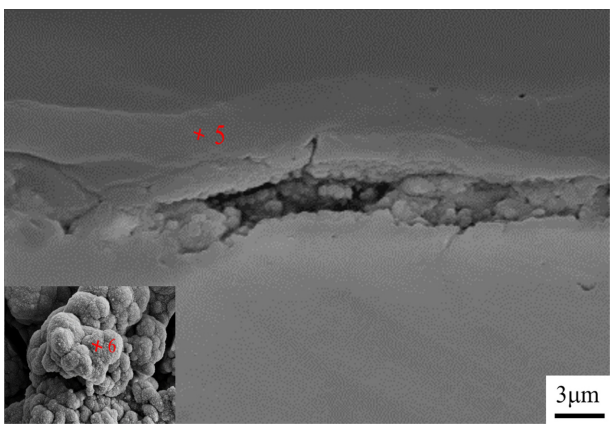

Fig. 10. Morphology of corrosion product layer in the black area of the blackened sample (reference for aluminum corrosion morphology)

Table 5. Composition of corrosion products on the cross section of the blackened sample and comparison with aluminum corrosion composition

Location	Al (at%)	Zn (at%)	Mg (at%)	O (at%)	Substance
5	37.66	12.71	0.49	49.14	Corrosion products of aluminum and zinc
6	22.73	1.2	0.6	75.47	Corrosion products of aluminum (as reference)

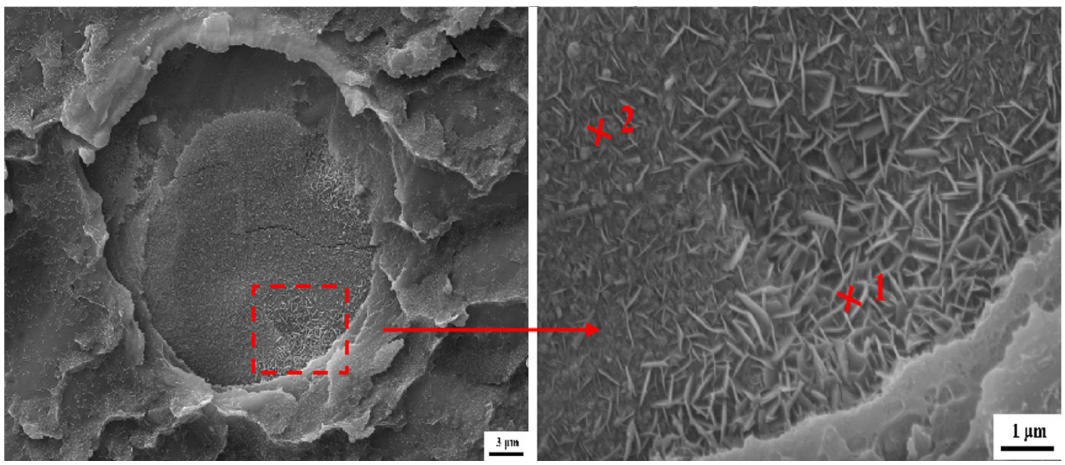

Fig. 11. Surface product morphology of the black area of the blackened sample after partial coating removal by the pulling method

Table 6. Composition of corrosion products in the black area of the drawing method blackboard

Location	Al (at%)	Zn (at%)	Mg (at%)	O (at%)	Cl (at%)	C (at%)	Si (at%)
1	20.42	17.74	4.47	33.77	0.07	23.33	0.2
2	32.58	7.31	4.45	35.71	0.07	17.57	2.31

After removing the fingerprint resistant coating from the black area of the blackened sample by using the pull-out method, it can be seen that a certain amount of corrosion product is present on the surface of the coating. Most of the corrosion products are needle shaped, with a small amount being spherical (Fig. 11), which might be assigned to the corrosion products of zinc and aluminum respectively. Based on EDS analysis (Table 6), it is speculated that the needle like structure at point 1 may be $Zn_5(OH)_6(CO_3)_2H_2O$, and the spherical shaped products at Point 2 may be Al $(OH)_3$. Further, it can be deduced that the corrosion of the zinc-rich phase had already occurred for a period of time, while the corrosion of the aluminum rich phase just begun.

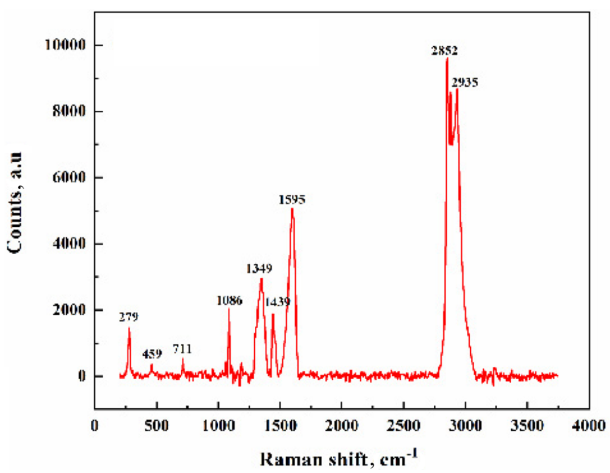

Fig. 12. Raman spectroscopic analysis results of zinc rich phase in the white area of the blackened sample

3.4 Raman spectroscopic detection of black transformation samples

Raman spectroscopy was performed on the white and black areas of the blackened sample to determine the corrosion products. From spectra results in Fig. 12 and Table 7, it can be seen that the corrosion undergone in the white area is relatively mild with only a small amount of Zn $(OH)_2$, indicating that the zinc-rich phase is corroded. Comparatively, the corrosion products in the black area were mainly composed of $Zn(OH)_2$, $Zn_5(OH)_6(CO_3)_2{\cdot}H_2O$, Mg $(OH)_2$ and $Al(OH)_3$, indicating that all alloy phases in the black area have undergone corrosion.

3.5 Analysis and discussion

In sum, all of the alloy phases in the black area of the blackened sample has undergone oxidation, and the oxygen content is significantly higher than that of the white area and normal sample. Comparatively, only zinc-rich phases were corroded for the white area, which can be attributed to a potential difference among those phases.

Table 7. Analysis results of corrosion products in different areas of the blackened sample plate

Name	Detection zone	Corrosion products
Blackening sample	Zinc rich phase in white area	ZnO, $Zn(OH)_2$
	Black area zinc rich phase	ZnO, $Zn(OH)_2$, $Zn_5(OH)_6(CO_3)_2{\cdot}H_2O$
	Aluminum rich phase in black area	a small amount $Mg(OH)_2$ and numerous $Al(OH)_3$

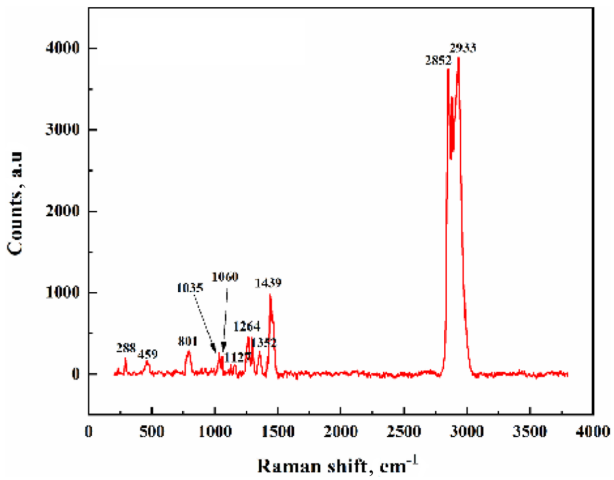

Fig. 13. Raman spectroscopic results of zinc rich phase in black region

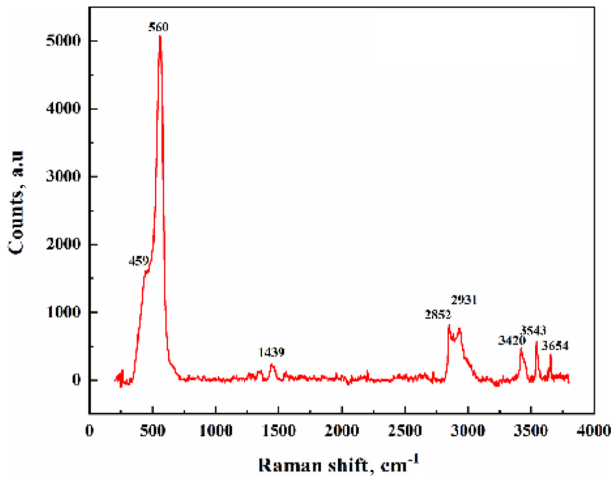

Fig. 14. Raman spectroscopic results of aluminum rich phase in the black region

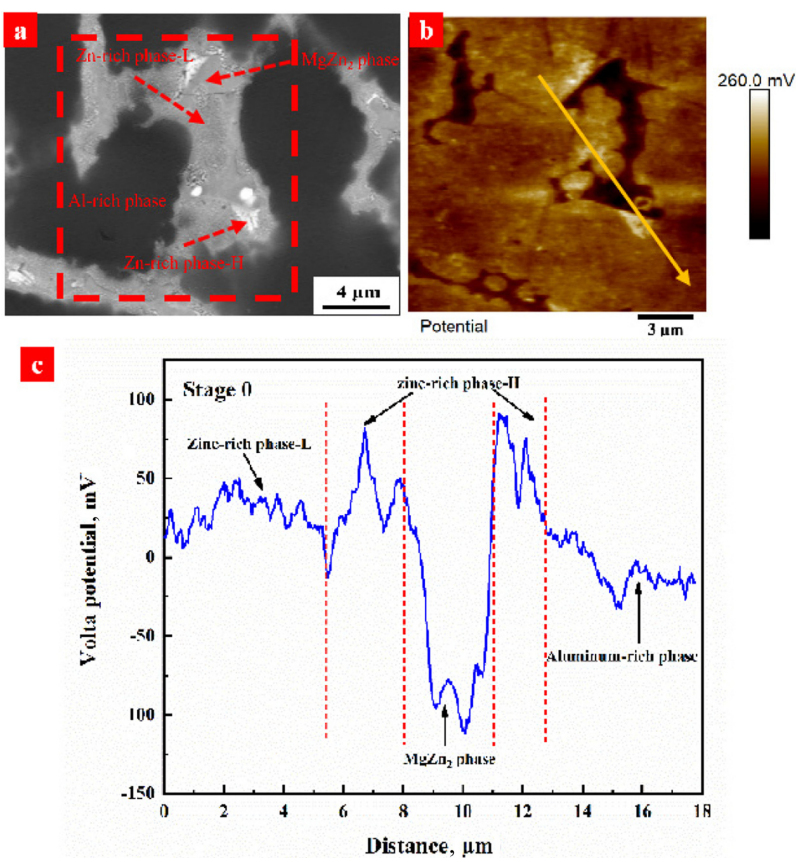

Fig. 15. Voltage-potential of different phases in aluminum zinc magnesium coating [1]

Based on the results of SKPFM, the Volta potential sequence of the original alloy phase is: $MgZn_2$ phase < aluminum rich phase < zinc rich phase - L < zinc rich phase-H (Fig. 15) [1]. In addition, according to an electrochemical test conducted by Šefl et al, neither η-Zn nor α-Al became anodic for 72 hours immersion. $MgZn_2$ and Mg_2Si were at least briefly anodic, acting as quick source of Mg^{2+} [2]. Therefore, in the presence of electrolytes such as water, the $MgZn_2$ phase in the coating is preferentially corroded as an anode.

It should be noticed that based on the potential sequence, the Al-rich phase in the original coating was the second negative, indicating that the Al-rich phase would be second only to the $MgZn_2$ phase to be preferentially corroded. However, the corrosion product of this phase was not detectable in the white area, where the zinc-rich phases was corroded. This unexpected result was attributed to the property of electrolyte. In the neutral NaCl solution electrolyte, given the easy formation of passive films and salt films on the surface of the Al-rich phase [3], the polarity of the Al-rich phase could be different from the polarity predicted by SKPFM in air [4,5].

4. Conclusion

1. The surface of the black area of the blackened sample has undergone oxidation, and the main difference in color difference between the samples is Δ L * value, which was negative.

2. There are different oxygen contents on the surface of the rich aluminum and zinc phases in the black area of the blackened sample, but both are higher than the white area and higher than the normal sample surface.

3. During the blackening process, the magnesium-contained phase preferentially dissolved, which is attributed to a relatively negative potential of $MgZn_2$ and Mg_2Si.

4. The black area of the blackened sample forms corrosion products under the fingerprint resistant film, including needle shaped products $Zn_5(OH)_6(CO_3)_2{\cdot}H_2O$ and spherical corrosion products $Al(OH)_3$.

5. The corrosion products in the black area were composed of $Zn(OH)_2$, $Zn_5(OH)_6(CO_3)_2H_2O$, $Mg(OH)_2$ and $Al(OH)_3$, and that in the white area were only a small amount of $Zn(OH)_2$.

References

1. J. Zou, Study on Corrosion Behavior and Mechanism of Alloy Phases in Al-Zn-Mg Coatings, unpublished master's thesis, University of Science and Technology Beijing, Beijing, China (2022).
2. V. Š. efl, T. Proš ek and Jan Š. vadlena, *Proc. 12th International Conference on Zinc and Zinc Alloy Coated Steel Sheet (Galvatech 2021Virtual Conference)*, p. 209, ISIJ, Shanghai, China (2021).
3. Z. Li, C. Li, Z. Gao, Y. Liu, X. Liu, Q. Guo, L. Yu, H. Li, Corrosion behavior of Al–Mg_2Si alloys with/without addition of Al–P master alloy, *Materials Characterization*, **110**, 170-174 (2015). Doi: https://doi.org/10.1016/j.matchar.2015.10.028
4. K. Yasakau, M. Zheludkevich, S. Lamaka and M. Ferreira, Role of intermetallic phases in localized corrosion of AA5083, *Electrochimica Acta*, **52**, 7651 (2007). Doi: https://doi.org/10.1016/j.electacta.2006.12.072
5. L. Lacroix, L. Ressier, C. Blanc and G. Mankowski, Statistical Study of the Corrosion Behavior of Al_2CuMg Intermetallics in AA2024-T351 by SKPFM, *Journal of the Electrochemical Society*, **155**, C8 (2008). Doi: https://doi.org/10.1149/1.2799089